Compression of shell targets heated by nanosecond pulses

N. G. Basov, P. P. Volosevich, E. G. Gamaliĭ, S. Yu. Gus'kov, A. A. Erokhin, Yu. A. Zakharenkov, N. N. Zorev, A. A. Kologrivov, V. B. Rozanov, A. A. Rupasov, A. A. Samarskiĭ, G. V. Sklizkov, and A. S. Shikanov

P. N. Lebedev Physics Institute, USSR Academy of Sciences
(Submitted 30 March 1979)
Zh. Eksp. Teor. Fiz. **78**, 420–430 (January 1980)

The dynamics of gas-filled shell targets irradiated by nanosecond laser pulses (the "compressing" shell regime), the heating and compression of deuterium when the shell collapse to the center, and the generation of thermonuclear neutrons are investigated. The shell velocity and time of collapse to the center in the "Kal'mar" facility are measured by various methods. The volume compression of the shells and the neutron yield are measured. The results of the experiments agree with the numerical calculations and with the theoretical model that establishes the laws of similarity of the physical processes.

PACS numbers: 52.50.Jm, 52.55.Pi

INTRODUCTION

The process of heating and compression of shell targets irradiated by nanosecond laser pulses in experiments with the "Kal'mar" facility at moderate laser radiation flux densities up to 10^{14} W/cm^2 (the "compressing shell" regime[1]) can be divided into two stages. The first is the formation of the laser-target corona (abporption and refraction of the heating radiation, heating and ionization of the corona material, formation of the corona density profile) was described in detail in a preceding paper.[1] The present paper deals with the second stage of the process, the shell motion induced by the reaction momentum of the corona, the energy transfer from the corona to the compressed thermonuclear matter, and the heating and compression of the latter.

1. SHELL MOTION DYNAMICS

The possibility of a quasi-stationary approach to the description of corona formation and shell dynamics[2,3] permits similarity laws to be established for the physical processes and to be used to derive the analytic dependences of the principal integral characteristics of the target compression and heating, such as the shell collapse time t^*, the average gas temperature $\overline{T}_g(t^*)$ and density $\rho_g(t^*)$, both averaged over the gas mass, at the instant of collapse, the neutron yield N, and of other characteristics on the initial parameters of the target and of the laser pulse. The equation of motion of the unevaporated part of the shell, assuming the latter to be infinitely thin, is of the form

$$M\frac{du}{dt}=4\pi R^2[P+\rho(v+u)^2-P_g], \quad u(t=0)=0. \tag{1}$$

Here u is the shell velocity, R is the coordinate of the evaporation boundary, P, ρ, and v are respectively the pressure, density, and velocity of the corona particles on the evaporation boundary, and P_g is the pressure of the compressed gas. The mass M is determined by the evaporation regime in accord with the formula

$$dM/dt=-4\pi R^2\rho_{sh}^0 D, \quad M(t=0)=M_0, \tag{2}$$

where ρ_{sh}^0 is the density of the unevaporated shell and the D is the velocity of the evaporation-wave front relative to the shell.

At neodymium-laser radiation flux densities $\leq 10^{14}$ W/cm^2 the state of the corona is close to one of the limiting cases of the previously considered model.[2] Namely, under these conditions the shell moves in such a way that during the greater part of the time the critical-density surface (ρ_{cr}), where the bulk of the laser energy is absorbed, and the Jouguet surface both lie near the evaporation boundary. Then, writing the conservation laws in the form

$$v+u+D=c, \tag{3}$$

$$\rho_{sh}^0 D=\rho_{cr}(v+u+D), \tag{4}$$

$$\frac{\dot{E}_{ab}}{4\pi R^2}=\rho_{cr}(v+u)\left[\varepsilon+\frac{P}{\rho}+\frac{(v+u)^2}{2}\right], \quad \varepsilon=\frac{P}{(\gamma-1)\rho}, \tag{5}$$

($\dot{E}_{ab}=dE_{ab}/dt$ is the average absorbed laser power and c is the speed of sound in the corona on the evaporation boundary), and recognizing that $D\ll u+v$, we obtain from these equations

$$\rho_{sh}^0 D=\rho_{cr}c, \tag{6}$$

$$P+\rho(v+u)^2=2\rho_{cr}c^2, \tag{7}$$

where

$$c=\left[\frac{2(\gamma-1)}{3\gamma-1}\left(\frac{\dot{E}_{ab}}{4\pi R_0^2\rho_{cr}}\right)\right]^{1/3}\left(\frac{R_0}{R}\right)^{1/3}=\tilde{c}\left(\frac{R_0}{R}\right)^{1/3}. \tag{8}$$

Thus, equations (1) and (2), with relations (6)–(8) taken into account, define completely the self-consistent problem of the callapse of a shell to the center under the influence of the evaporated-mass momentum. The solution of Eqs. (1) and (2) with account taken of (6)–(8) during the shell-acceleration stage [$P_g\ll P+\rho(v+u)$ takes in the approximation where $\dot{E}_{ab}\approx$ const the form

$$u=\tilde{u}\left(\frac{M_0}{M^*}\right)^{1/5}\left[1-\left(\frac{R(t)}{R_0}\right)^{5/3}\right]^{1/3}, \quad \tilde{u}=\left(\frac{12}{5}\right)^{1/5}\left(\frac{R_0\rho_{cr}}{\Delta_0\rho_{sh}^0}\right)^{1/3}\tilde{c}; \tag{9}$$

$$M^*=M(t^*)=C_1M_0\left[1-\left(\frac{\overline{M}}{M_0}\right)^{1/5}\right]^2, \quad \overline{M}=\frac{5}{48}\left(\frac{R_0\rho_{cr}}{\Delta_0\rho_{sh}^0}\right)M_0. \tag{10}$$

Here R_0 and Δ_0 are the initial radius and initial thickness of the shell.

 0038-5646/80/010212-06$02.40 © 1980 American Institute of Physics

Since the time of deceleration of the shell by the compressed gas is much shorter than the acceleration time, the collapse time t_a^* is determined with sufficient accuracy by integrating Eq. (9) and is equal to

$$t_a^* \approx C_2 \left(\frac{5}{12}\right)^{1/2} \frac{\pi}{2} \left(\frac{M^*}{M_0}\right)^{1/2} \frac{R_0}{\bar{c}} \left(\frac{R_0\rho_{cr}}{\Delta_0\rho_{sh}^0}\right)^{-1/2}. \quad (11)$$

The hydrodynamic-coupling coefficient $\eta = E_{kin}/E_{ab}(t^*)$ takes according to (11) the form

$$\eta \approx C_3^2 \frac{\gamma-1}{3\gamma-1} \left[\left(\frac{12}{5}\right)^{1/2} \frac{1.43}{\pi}\right]^3 \left(\frac{R_0\rho_{cr}}{\Delta_0\rho_{sh}^0}\right)^{1/2} \left(\frac{M_0}{M^*}\right)^{1/2}. \quad (12)$$

The obtained solutions contain only one dimensional parameter $\bar{c}$, the scale of the speed of sound on the discontinuity, and the dimensionless parameter $R_0\rho_{cr}/\Delta_0\rho_{sh}^0$, which has a clear physical meaning—the ratio of the accelerating and accelerated surface masses.

Thus, the similarity laws (9)–(12) determine the dependences of the principal characteristics of the shell dynamics on the initial parameters of the target and of the laser pulse. Comparison with numerical calculations by the "Luch" program,[1] which simulate the experiments with the Kal'mar facility, shows that Eqs. (9)–(12) yield results close to the calculated ones if the constants C_1, C_2, and C_3 equal respectively 0.8, 1.4, and 1.6.

It is of interest to note the interrelation between the shell dynamics and the hydrodynamic processes in the corona. This interrelation can be used to investigate the dynamics of the unevaporated part of the shell, by studying the processes that occur in the plasma corona—that part of the laser plasma which is presently easiest to diagnose experimentally for the compressed-shell regime. Thus, we have previously pointed[1] to the possibility of determining the shell collapse time by measuring the velocity of the shock wave that emerges from the corona after reflection from the center of the target and passing through the unevaporated part of the shell. In the present study we investigate the dynamics of target compression by using also the plasma emission at double the frequency of the heating light, as well as x-ray emission.

It is known that second-harmonic generation takes place in the laser-target corona near the critical-density surface ($n_{cr} = 10^{21}$ cm^{-3} for neodymium-laser emission).[4] As already indicated, at a weak time dependence of the laser radiation flux the motions of the critical-density surface and of the unevaporated part of the shell are correlated. Thus, using the $R-t$ diagram of the motion of the critical-density surface, a diagram determined from the time scan of the image of the second harmonic of the plasma luminosity region,[5,6] it is possible to investigate the dynamics of the motion of the unevaporated part of the shell itself, and in particular, to determine the time of its collapse. For an experimental determination of the $R-t$ diagram of motion of the critical-density surface, the image of the plasma in the light of the $2\omega_0$ harmonic, which was separated by a set of light filters, was projected on the slit of a photoelectronic recorder. Figure 1 shows typical $R-t$ diagrams of the motion of the critical-density surface, obtained by reducing the streak photographs of the plasma taken in $2\omega_0$ light. During the stage of corona formation, when the shell velocity is low, the critical-density surface moves outward relative to the initial position of the outer target boundary, and then starts moving towards the center. During the stage of expansion of the unevaporated part of the shell, the critical-density surface again moves away from the center. The instant of time $t(R_{cr}^{min})$ corresponding to the minimum value of the critical-surface radius on the $R-t$ diagram is uniquely connected with the instant of shell collapse $t^* = t(R_{cr}^{min}) + \delta t$, where δt is the time at which the perturbation reaches the critical surface after the stopping of the inner boundary of the shell. In order of magnitude, δt is equal to the ratio of the shell thickness Δ to the speed of sound in the compressed shell. Numerical calculation yields for δt, under the conditions of the experiments discussed here, values $(0.1-0.15)\times10^{-9}$ sec.

The table lists the shell-collapse times t_{exp}^*, determined by the procedure described above in six experiments,[3] as well as the values t_{calc}^* obtained in numerical calculations using the "Luch" program and t_a^* obtained from formula (11). It is seen from these data that Eq. (11), obtained within the framework of a simple hydrodynamic model, accounts correctly for the dependence of t^* on the shell parameters and on the absorbed energy. The good agreement with the theoretical results indicates that the pressure of the corona and the unevaporated mass of the shell were close to the calculated values in the experiments. In the calculations the pressure near the surface with ρ_{cr} was 10^5-10^6 atm, $T_e(R_{cr}) \approx 0.5-0.7$ keV, the average degree of ionization ~10, $M^* \approx (60-70)\%M_0$, and the coefficient of the hydrodynamic transfer was $\eta \approx 5-10\%$. The corona temperature determined in the experiment was also 0.5–0.7 keV.

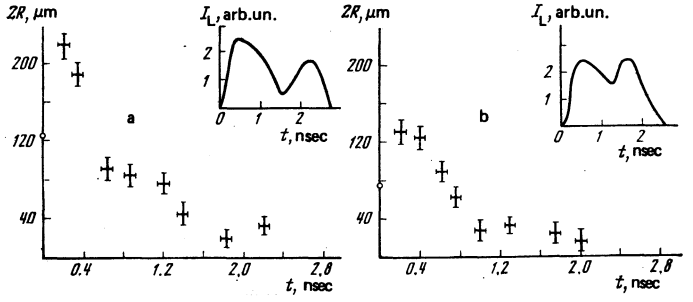

FIG. 1. Dynamics of the motion of the critical region during the shell contraction stage: a—$2R = 125$ μm, $\Delta = 2.1$ μm, $P_D = 15$ atm; b—$2R = 75$ μm, $\Delta = 0.9$ μm, $P_D = 15$ atm. In the upper right corner is shown the waveform of the heating pulse, I_L is the intensity of the laser radiation.

To investigate the time evolution of the pressure distribution in the target, it is important to study the stage of expansion of the unevaporated part of the shell. Figure 2 shows $R-t$ diagrams of the motion of the inner boundary of the shell and the time dependences of the ratio of the pressures of the compressed gas and of the corona during the expansion stage, obtained in calculations by the "Luch" program under conditions of experiments whose $R-t$ diagrams are shown in Fig. 1. An interesting singularity is possessed by the expansion of the second, lighter, shell (Fig. 2b), the collapse-time of which $t^* \approx 1$ nsec is much less than the duration of the laser pulse. By the end of termination of the action of the pulse it manages to be compressed again. The agreement between the experimental and calculated $R-t$ diagrams suggests that the distribution of the pressures in the target is close to the calculated one.

The shell dynamics was investigated also using time-resolution measurements of the emission spectrum of the $2\omega_0$ harmonic generated in the plasma in the region of the critical density.[7] The shift $\Delta\lambda_{2\omega_0}$ (relative to the nominal value $\lambda_0/2$) of the fundamental component of the spectrum of the harmonic produced by the linear transformation of the heating radiation into longitudinal plasma waves, is due to the Doppler effect produced when the generation region moves.[8] Therefore measurement of the dependence of the shift $\Delta\lambda_{2\omega_0}$ on the time makes it possible to reconstruct the time evolution of the rate of motion of the region of the critical density of the plasma.

Figure 3 shows the $v-t$ diagram obtained from measurements of the temporal evolution of the second-harmonic spectrum in one of the experiments. The time evolution of the described methods of the measurement of the $R-t$ and $v-t$ diagrams of the motion of the critical-density surface is less than 0.1 nsec. The maximum shell velocity towards the target center measured in this manner in the various experiments varied in the range $(3\times10^6-10^7)$ cm/sec, while the quantity $t^* \sim R_0/v_{max}$ varied with the target parameters in accordance with Eq. (11).

Important information on the shell motion is obtained by investigating the x radiation of the plasma. Figure 4

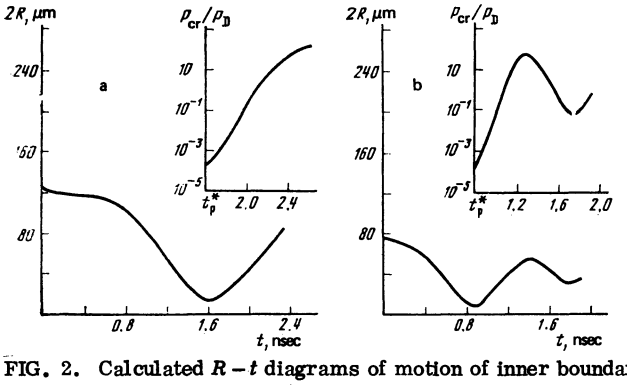

FIG. 2. Calculated $R-t$ diagrams of motion of inner boundary of shells: a—$2R=125$ μm, $\Delta=2.1$ μm, $P_D=15$ atm; b—$2R=75$ μm, $\Delta=0.9$ μm, $P_D=15$ atm. In the upper corner is shown the temporal evolution of the ratio of the pressures in the corona and in the compressed matter of the target.

TABLE I.

Number of experiment	Shell parameters: $2R_0$, μm	Δ, μm	P_D, atm	E_{ab}, J	t^*_{exp}, nsec	t^*_{calc}, nsec	t^*_a, nsec: Eq. (1)
1	125	2.25	0	15±3	1.5±0.15	1.5	1.02
2	125	2.1	15	9±1.5	1.8±0.15	1.7	1.1
3	100	1.2	0	13±2.5	1.25±0.12	1.1	0.75
4	98	1.4	0	12±2	1.4±0.15	1.3	0.86
5	90	1.1	22	11±2	1.1±0.1	0.95	0.66
6	75	0.9	15	10±2	0.9±0.1	0.8	0.53

Note. In the table, P_D is the deuterium pressure, E_{ab} is the absorbed energy, t^*_e is the experimentally determined shell-collapse time, t^*_{calc} and t^*_a are the values determined by numerical calculation and from Eq. (11).

shows a soft-x-ray pinpoint photograph of the plasma emission in an experiment in which the targets were illuminated with a specially shaped laser pulse having two intensity maxima separated 0.7–0.8 nsec in time and with a dip $I_{max}/3$ between them. The time waveform of the pulse was registered with a moving image camera with a time resolution ~0.1 nsec. The two concentric external rings on the pinpoint photograph correspond to the arrival of the laser-radiation intensity maxima at the plasma. The central region of the pinpoint photograph corresponds to the emission of the compressed nucleus. Since the main contribution to the plasma x-ray luminosity is made by a region with density close to critical, the use of a laser pulse of special waveform to irradiate the target yields two points of the $R-t$ diagram. However, the practical use of these two $R-t$ diagram points, for example to determine the average shell velocity, should be approached with some caution, since the second and later point of the $R-t$ diagram can belong to the stage of expansion of the shell after the instant of the collapse.

For the described experiment, which demonstrates the method, estimates based on Eq. (11) yield for the collapse time a value exceeding the time of arrival of the second maximum of the heating point at the plasma. The average rate of collapse of the shell

$$u=[R(t_1)-R(t_2)]/(t_2-t_1)$$

(where the times t_1 and t_2 correspond to the first and second maxima of the pulse) turns out to be 3×10^6 cm/sec.

Figure 5 shows the dependence of the radius of the

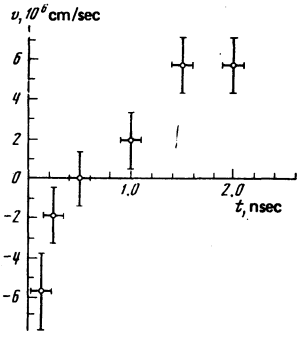

FIG. 3. $v-t$ diagrams of the velocity of motion of the region of the critical density for a target of diameter $2R=163$ μm with wall thickness $\Delta R=4.6$ μm.

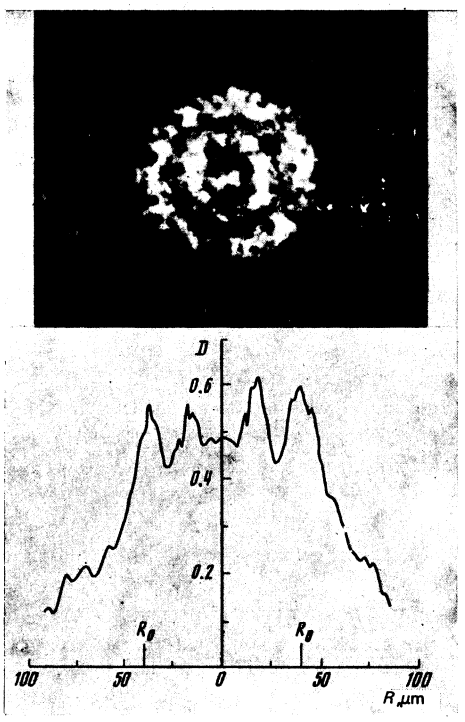

FIG. 4. x-ray pinpoint photograph and photographic density profile of its diametral section for a target of diameter $2R = 80$ μm with wall thickness $\Delta R = 1.5$ μm, irradiated with a double laser pulse.

outer luminous annular region on the thickness of the shell in the time-integrating pinpoint photographs obtained in experiments with a single laser pulse. This dependence is the result of the change of the dynamics of the motion of the shell and of the critical surface with changing shell thickness. According to the results obtained in the present paper and according to the conclusions of Ref. 2, the distance to which the region of the critical density moves away from the surface of the target the time interval required for the reversal of its direction of motion, and also the total time of collapse, all increase with increasing thickness of the shell wall. By the instant of arrival of the maximum laser-pulse intensity at the target $[t(I_{max}) \sim 0.5$ nsec] the region with the critical density is located at different distances from the initial radius of the shell in the case of shells with different wall thicknesses. In accord with the indicated singularities of the $R-t$ diagrams, the motions of this region lead to the dependence plotted in Fig. 5.

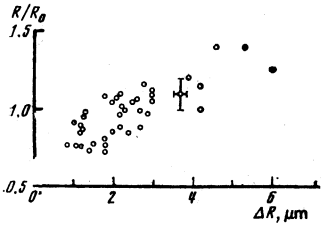

FIG. 5. Dependence of the ratio of the diameter of the outer luminous region of the x-ray pinpoint photographs to the initial diameter of the targets on the wall thickness.

2. HEATING AND COMPRESSION OF DEUTERIUM. NEUTRON YIELD

The simple geometric model of shell motion, considered in the preceding section, does not take into account the stage of shell deceleration, when the pressure in the corona becomes less than the pressure of the compressed gas. During this stage, by the instant of shell collapse, the enitre kinetic energy of the shell goes over into the internal energy of the compressed gas $\varepsilon_g(t^*)$ and of the shell $\varepsilon_{sh}(t^*)$:

$$\eta E_{ab}(t^*) = \varepsilon_g(t^*) + e_{sh}(t^*).$$

At the instant of shell collapse it can be assumed that the gas pressure $\overline{P}_g(t^*)$ and the shell pressure $\overline{P}_{sh}(t^*)$ are approximately equal: $\overline{P}_g(t^*) \approx \overline{P}_{sh}(t^*)$. Assuming furthermore that the target material is an ideal gas, we obtain for the average gas temperature the equation

$$\overline{T}_g(t^*) = \eta E_{ab}(t^*) \Big/ A_g m \left[1 + \frac{4}{3}\frac{\delta_g(t^*)}{\delta_{sh}(t^*)}\frac{\rho_g^0}{\rho_{sh}^0}\frac{M^*}{m}\right], \tag{13}$$

in which m is the gas mass, A_g is its specific heat, and ρ_g^0 and ρ_{sh}^0 are the initial densities of the gas and of the shell. The degrees of compression of the gas and of the shell, $\delta_g(t^*)$ and $\delta_{sh}(t^*)$, are determined by schematically representing the compression of the shell as consisting of two stages: the passage of the shock wave through the shell and the gas, and their subsequent adiabatic additional compression. As a result we get

$$\delta_g(t^*) = \frac{\rho_g(t^*)}{\rho_g^0} \approx C_4 \cdot 20 \left[M^*/m \left(1 + \frac{4}{3}\frac{\delta_g(t^*)}{\delta_{sh}(t^*)}\frac{\rho_g^0}{\rho_{sh}^0}\frac{M^*}{m}\right)\right]^{1/(\gamma-1)},$$
$$\delta_g(t^*)/\delta_{sh}(t^*) \approx C_5 (1+\sqrt{5})^{-2/\gamma} (\rho_{sh}^0/\rho_g^0)^{1/\gamma}. \tag{14}$$

$\gamma = 5/3$ is the adiabatic exponent. Equations (13) and (14), with (12) taken into account, determine the similarity laws for the temperature and density of the target at the instant of collapse when the initial conditions of the compressing-shell regime are changed. They yeild values close to the results of the numerical calculations by the "Luch" program, with the coefficients C_4 and C_5 equal to 1.50 and 1.45, respectively.

The number of thermonuclear neutrons produced in a spherically symmetrical deuterium plasma is

$$N_{DD} = \int_0^\infty \int_0^{R(t)} \frac{n^2(r,t)}{2} \langle \sigma u \rangle_{DD} 4\pi r^2 dr\, dt. \tag{15}$$

Here $n(r,t)$ is the plasma density, $\langle \sigma v \rangle_{DD}$ is the cross section of the D + D reaction, averaged over the Maxwellian distribution, and can be expressed approximately in the power-law form $\langle \sigma v \rangle_{DD} = AT^k$.

The temperature of the compressed deuterium ranged in the experiments in question from 0.1 to 1.0 keV, with a very strong temperature dependence of the cross section of the D + D reaction. Therefore practically all the neutrons are produced during a short time interval near the instant of maximum compression. Inasmuch as in this case the pressure of the compressed deuterium greatly exceeds the pressure of the corona, the equation of motion of the shell during the stages of the adiabatic compression and expansion of the gas takes the form ($\gamma = 5/3$)

$$M\frac{du}{dt} = \pm 4\pi R^2 P_g, \quad P_g(t) = P_g(t^*)\left[\frac{R(t^*)}{R(t)}\right]^5$$

Solution of this equation yields the following time dependences of the mean values of the temperature and the density of the gas during the neutron-production stage:

$$\bar{T}_g(t)=\bar{T}_g(t^*)\left[1+\left(\frac{t-t^*}{\tau}\right)^2\right]^{-1},$$
$$\rho_g(t)=\bar{\rho}_g(t^*)\left[1+\left(\frac{t-t^*}{\tau}\right)^2\right]^{-3}, \quad (16)$$

in which the characteristic time of inertial containment is

$$\tau=\frac{R(t^*)}{c_g(t^*)}\left(\frac{M^*}{3m}\right)^{1/2},$$

and $c_g=[\frac{2}{3}A_g\bar{T}_g(t^*)]^{1/2}$ is the speed of sound at the instant of collapse t^*. The spatial distribution of the temperature and of the density of the deuterium can be approximately determined from the condition that the flux of the electron thermal conductivity be constant

$$\varkappa T_g^{5/2}\frac{\partial T_g}{\partial r}\approx \text{const}$$

and that the gas pressure become equalized $\partial P_g/\partial r\approx 0$:

$$T_g(r,t)=T_g(0,t)\,(1-r/R)^{2/5}, \quad \rho_g(r,t)=\rho_g(0,t)\,(1-r/R)^{-3/5},$$
$$T_g(0,t)=1.8\bar{T}_g(t), \quad \rho_g(0,t)=\bar{\rho}_g(t)/1.8. \quad (17)$$

Substituting the expressions of (17), with allowance for (16), in Eq. (15) and integrating, we obtain

$$N_{DD}\approx 3\cdot 10^{46}\tau\frac{\pi^{1/2}}{4}\left[\frac{257}{(k+3/2)(k+5)(k+17/2)}m\right]\bar{\rho}_g(t^*)\langle\sigma v\rangle|_{T_g=1.8\bar{T}_g(t^*)}. \quad (18)$$

In the experiments with the "Kal'mar" facility, the neutron radiation was registered both with scintillation detectors and multipliers, located at various distances from the target, and with an integral indium activation detector. Time-of-flight measurements performed with three scintillation detectors have shown that the energy of the neutrons produced upon compression of the glass shell targets filled by deuterium gas corresponds to the energy of the neutrons produced as a result of the D + D reaction. This confirms the thermonuclear origin of the registered neutron radiation. Most experiments with the gas-filled targets were performed for shells with small diameters, $2R_0 \leq 100$ μm, and in these experiments the neutron yeild, which was not stable, reached 10^2–10^4 particles per shot. The maximum neutron yield $N\sim 3\times 10^6$ neutrons was registered for a glass shell target of diameter $2R_0\approx 140$ μm with wall thickness $\Delta_0\approx 2.2$ μm at an initial deuterium pressure $P_g^0\approx 35$ atm.[6]

The cause of the instability of the neutron yeild in the experiments with the "Kal'mar" facility is the very high sensitivity of its value to the initial parameters of the target and to the experimental conditions. An analysis of the analytic model and of the numerical calculations by the "Luch" program shows that as a result of the strong temperature dependence of the rate of the thermonuclear reaction at $T < 1$ keV, for example, an increase of the absorbed energy from 20 to 30 J or a decrease of the initial pressure of the deuterium from 35 to 15 atm leads to an increase of the neutron yield by an order of magnitude. In addition, according to (18), the main contribution to the formation of the thermonuclear neutrons is made by a small central mass of deuterium (~20–30% m) with temperatures close to the maximum of the spatial distribution (17). Therefore, if as a result of the compression asymmetry (due to the inhomogeneity or to variation in the shell thickness, or else due to the insufficient inhomogeneity of the irradiation by the laser) the maximum of the spatial distribution of the temperature is not realized, the neutron yield can be substantially lower than expected. The problem of the neutron yield under conditions of a compressing shell, at an absorbed-energy level ≤50 J, will be considered in a separate article.

The volume compression of the deuterium was determined in the "Kal'mar" experiments by recording the continuous x radiation of the plasma with pinpoint cameras having a spatial resolution 10 μm. Figure 6 shows a pinpoint photograph of the plasma taken in its own x rays ($\hbar\nu\sim 2$ keV), for a glass shell target with diameter $2R_0\approx 140$ μm and wall thickness $\Delta_0\approx 2.2$ μm, filled with deuterium with initial pressure $P_g^0\sim 35$ atm. In addition to the outer luminous region, which corresponds to the expanding plasma corona, one can see an inner annular structure—a luminous layer of glass adjacent to the compressed gas. This makes it possible to determine the volume compression of the gas δ_g. The pressure of the deuterium compressed as a result of the collapse of the shell can be estimated from measurements of the instant of time of the secondary collapse in the case when the time of the first collapse of the shell is much less than the duration of the laser pulse.

Indeed, the dynamics of the expansion of the shell after the first collapse is determined by the ratio of the pressures in the corona and in the compressed matter of the target. The average pressure in the corona is determined from the experimental investigation of the corona parameters. In addition, it can be estimated from the similarity relations of the present paper, using Eqs. (7) and (8). The temporal evolution of the pressure of the compressed target material is determined by the adiabatic expansion and is expressed in terms of the pressure at the instant of the first collapse. The described procedure for the experiment

FIG. 6. X-ray pinpoint photographs for a target of diameter $2R = 140$ μm with wall thickness $\Delta R = 2.2$ μm and initial deuterium pressure $P_D = 35$ atm.

whose $R-t$ diagram is shown in Fig. 1b, yields at the secondary-collapse time $t^* \sim 1.8$ nsec a deuterium pressure $P(t^*) \approx 10^9$ atm. The deuterium pressure determined in this manner, together with the x-ray procedure for determining the volume compression, permits an indirect conclusion to be drawn concerning the deuterium temperature, which under the indicated experimental conditions amounted to ~0.2–0.4 keV. In a run of experiments with shell parameters $2R_0 \approx 120$–140 μm and $\Delta_0 \sim 2$–3 μm, and at a pressure of the contained deuterium 30–35 atm, the volume compression amounted to $\sim 10^3$, corresponding to a compressed-deuterium density $\rho_g(t^*) \sim 6$–8 g/cm^3 and to a parameter $\rho_g R \approx 5 \times 10^{-3}$ g/cm^2. These results agree well with calculations by the "Luch" program and with estimates based on (14), which predict under the indicated experimental conditions $\rho_g(t^*) \approx 4$–7 g/cm^3. This agreement allows us to state that in the "Kal'mar" experiments the heating and compression of the shells actually do take place in the compressing-shell regime, a distinguishing feature of which is the introduction of the initial entropy into the compressed target material only by the shock wave without preliminary heating by fast electrons and by thermal conductivity.

CONCLUSION

The results of the investigations reported in the present article and in Ref. 1 allow us to present a self-contained picture of the process of heating and compression of laser targets in the compressing-shell regime. At a laser energy ~100 J and at radiation flux densities $\sim 10^{14}$ W/cm^2, in shell of 100–200 μm, approximately 20–30% of the energy is absorbed.[1] The main contribution is made then by the inverse bremsstrahlung process. The use of a classical Spitzer thermal conductivity in the hydrodynamic model at the indicated value of the absorbed energy makes it possible to present, in the numerical calculations and in the theoretical analysis, a discription of the state and of the dynamics of the laser-target corona which is close to the experimental situation. This manifests itself particularly clearly in the identification, with the aid of numerical calculations, of the experimentally registered perturbations of the laser-target density profile by the shock wave reflected from the center.[1] In this model it is also possible to describe well the dynamics of the compression of the unevaporated part of the shell, which leads to satisfactory agreement between the experimental and theoretical $R-t$ diagrams of the critical surface, and also of the times of compression at various parameters of the target and of the laser pulse. Thus, according to our interpretation, the hydrodynamics with classical absorption of the laser radiation and electron thermal conductivity is an adequate method of describing the compression and heating of the target at moderate fluxes.

It must be noted that the state of the compressed and heated core of the target (the distribution of the density and of the temperature, the degree of penetration of the shell matter into the gas) depends strongly on the initial asymmetry of the shell and of the irradiation, which are presently not known with sufficient accuracy and are the subject of further experimental and theoretical investigations.

[1] Yu. V. Afanas'ev, N. G. Basov, B. L. Basin, P. P. Volosevich, E. G. Gamalii, S. Yu. Gus'kov, N. N. Demchenko, Yu. A. Zakharenkov, N. N. Zorev, A. A. Kologrivov, V. B. Rozanov, A. A. Rupasov, A. A. Samarskii, G. V. Sklizkov, and A. S. Shikanov, Zh. Eksp. Teor. Fiz. **77**, 2539 (1979) [Sov. Phys. JETP **50**, 1229 (1979)].

[2] Yu. V. Afanas'ev, E. G. Gamaliĭ, O. N. Krokhin, and V. B. Rozanov, Zh. Eksp. Teor. Fiz. **71**, 594 (1976) [Sov. Phys. JETP **44**, 311 (1976)].

[3] N. G. Basov, P. P. Volosevich, E. G. Gamaliĭ, S. Yu. Gus'kov, Yu. A. Zakharenkov, O. N. Krokhin, V. B. Rozanov, G. V. Sklizkov, and A. S. Shikanov, Pis'ma Zh. Eksp. Teor. Fiz. **28**, 135 (1978) [JETP Lett. **28**, 125 (1978)].

[4] V. P. Silin, Parametricheskoe vozdeĭstvie izlucheniya bol'shoĭ moshchnosti na plazmu (Parametric Action of High-Power Radiation on a Plasma), Nauka, 1973.

[5] Yu. A. Zakharenkov, O. N. Krokhin, G. V. Sklizkov, and A. S. Shikanov, Kvantovaya Elektron. (Moscow) **3**, 1068 (1976) [Sov. J. Quantum Electron. **6**, 571 (1976)].

[6] N. G. Basov, A. A. Erokhin, Yu. A. Zakharenkov, N. N. Zorev, A. A. Kologrivov, O. N. Krokhin, A. A. Rupasov, G. V. Sklizkov, and A. S. Shikanov, Pis'ma Zh. Eksp. Teor. Fiz. **26**, 581 (1977) [JETP Lett. **26**, 433 (1977)].

[7] V. Yu. Bychenkov, Yu. A. Zakharenkov, O. N. Krokhin, A. A. Rupasov, V. P. Silin, G. V. Sklizkov, A. N. Starodub, V. T. Tikhonchuk, and A. S. Shikanov, Pis'ma Zh. Eksp. Teor. Fiz. **26**, 500 (1977) [JETP Lett. **26**, 364 (1977)].

[8] N. G. Basov, V. Yu. Bychenkov, O. N. Krokhin, M. V. Osipov, A. A. Rupasov, V. P. Silin, G. V. Sklizkov, A. N. Starodub, V. T. Tikhonchuk, and A. S. Shikanov, Preprint Fiz. Inst. Akad. Nauk SSSR, No. 256, 1978.

Translated by J. G. Adashko